CORE
Metadata, citation and similar papers at core.ac.uk
Provided by Sissa Digital Library

Journal of Physics: Conference Series

PAPER • **OPEN ACCESS**

Simulation of electron energy loss spectra with the *turboEELS* and *thermo_pw* codes

To cite this article: Oleksandr Motornyi *et al* 2018 *J. Phys.: Conf. Ser.* **1136** 012008

View the article online for updates and enhancements.

IOP ebooks™

Bringing you innovative digital publishing with leading voices to create your essential collection of books in STEM research.

Start exploring the collection - download the first chapter of every title for free.

This content was downloaded from IP address 147.122.97.141 on 20/02/2019 at 09:46

IOP Conf. Series: Journal of Physics: Conf. Series **1136** (2018) 012008 doi:10.1088/1742-6596/1136/1/012008

Simulation of electron energy loss spectra with the *turboEELS* and *thermo_pw* codes

Oleksandr Motornyi[1], Michèle Raynaud[1], Andrea Dal Corso[2], Nathalie Vast[1]

[1] Laboratoire des Solides Irradiés, École Polytechnique - CEA DRF IRAMIS - CNRS UMR 7642, Paris-Saclay University, 91128 Palaiseau cédex, France
[2] Scuola Internazionale Superiore di Studi Avanzati (SISSA), Via Bonomea 265, IT-34136 Trieste, Italy, IOM-CNR Trieste, Italy

E-mail: oleksandr.motornyi@polytechnique.edu

Abstract.

For some materials like noble metals, electron energy loss spectra have a complex structure that makes them difficult to analyze without the help of *ab initio* calculations. Various theoretical approaches can be used for this purpose, among which the time-dependent density functional perturbation theory (TDDFPT) which has been widely used to study plasmons in a number of bulk and surface systems. In the present paper we present a comparison of the results and performance of two different numerical implementations of TDDFPT: the Sternheimer and Liouville-Lanczos methods. The former approach is implemented in the *thermo_pw* module and the latter one in the *turboEELS* code of the QUANTUM ESPRESSO package for electronic structure calculations. In the present paper a comparison is made for bulk bismuth, a semimetal, taking into account spin-orbit coupling, as well as for bulk gold, a noble metal. We show that for these two examples, both codes gives identical results and the *turboEELS* code has a better performance than the *thermo_pw* code, and point out in which cases the usage of *thermo_pw* alone or of both codes can be advantageous.

1. Introduction

Electron energy loss (EEL) spectroscopy [1] is a powerful experimental method that allows one to measure the change in kinetic energy -the energy loss- of electrons after their interaction with a sample. This technique can be used to obtain structural and chemical information about a specimen -from the high-energy loss region of the spectra- as well as information about valence electron excitations -from the low-energy loss region of the spectra-. In particular, the valence region of the spectra contains information about the band structure and dielectric properties of the material: plasmons, surface plasmons and interband transitions. For some materials like aluminum, valence EEL spectra has a simple structure containing one single, well-defined, plasmon peak for which the Drude model is a pertinent approximation. In materials where the behavior of valence electron is far from the (quasi) free electron model however, the EEL spectrum contains many peaks from single, to collective and to superposition of collective and single excitations, that make it difficult to analyze.

In order to perform a thorough analysis it is convenient to simulate EEL spectra computing the dielectric function. Indeed, in an EEL spectroscopy experiment, the inelastic scattering

Content from this work may be used under the terms of the Creative Commons Attribution 3.0 licence. Any further distribution of this work must maintain attribution to the author(s) and the title of the work, journal citation and DOI.
Published under licence by IOP Publishing Ltd

probability of an incoming electron by the electrons of the solid, given by the double-differential cross-section $d^2\sigma/(d\omega d\Omega)$ is measured, which is linked to the macroscopic dielectric function ϵ_M:

$$\frac{d^2\sigma}{d\omega d\Omega} \sim Im[\frac{1}{\epsilon_M(\mathbf{Q},\omega)}], \tag{1}$$

where $\mathbf{Q}$ is a momentum transfer, ω is an electron energy loss, and $d\Omega$ is the elemental solid-angle in which the scattering occurs.

Various *ab initio* methods that allow one to calculate spectral properties of solids have been developed in the past decades, addressing different aspects of the problem [2]. Time-dependent density functional theory (TDDFT) has been widely used to study plasmons in a number of bulk and surface systems [3, 4]. We note however that even for a material as simple as covalent silicon, one might need to account for many-body (excitonic) effects beyond TDDFT for instance to properly describe the shape of the plasmon peak [5].

In the present paper we will focus on the time-dependent density functional perturbation theory (TDDFPT) and linear response approach [6, 7] to the calculation of the dielectric function. Two implementations, the Sternheimer and Liouville-Lanczos methods, will be compared for bulk bismuth and gold. The paper is organized as follows. In Sec. 2, a brief overview and comparison of the theoretical methods: classic TDDFT approach, and the Liouville-Lanczos and Sternheimer approaches to TDDFPT, will be given. In Sec. 3, results obtained using different approaches and corresponding implementations will be shown along with the comparison of the performance of the codes. Finally, conclusions will be drawn in Sec. 4.

2. Comparison of theoretical approaches to linear response calculations

2.1. Dyson-like equation

The dielectric function in eq. (1) is determined by the macroscopic density response function (or susceptibility) χ_M [8]:

$$\epsilon_M(\mathbf{Q},\omega)^{-1} = 1 + v_G(\mathbf{Q})\chi_M(\mathbf{Q},\omega), \tag{2}$$

where $v_G(\mathbf{Q}) = 4\pi e^2/|\mathbf{Q}|^2$ is the Fourier transform of the Coulomb potential. χ_M is related to the microscopic density response function $\chi_{\mathbf{G},\mathbf{G}}(\mathbf{q},\omega)$:

$$\chi_M(\mathbf{Q},\omega) = \chi_{\mathbf{G},\mathbf{G}}(\mathbf{q},\omega), \tag{3}$$

where $\mathbf{Q} = \mathbf{q} + \mathbf{G}$, with $\mathbf{G}$ being a reciprocal lattice vector and $\mathbf{q}$ a wavevector in the first Brillouin zone. Within the traditional linear response approach of TDDFT, χ of the interacting many-body system is related to the density response function χ^0 of the non-interacting Kohn-Sham (KS) system through a Dyson-like screening equation:

$$\chi = \chi^0 + (v + f_{xc})\chi. \tag{4}$$

f_{xc} is the exchange-correlation kernel and χ^0 is given by

$$\chi^0_{\mathbf{G},\mathbf{G}'}(\mathbf{q},\omega) = \frac{1}{V}\sum_{\mathbf{k}}^{BZ}\sum_{n,n'}\frac{f_{n,\mathbf{k}} - f_{n',\mathbf{k}+\mathbf{q}}}{\hbar\omega + \varepsilon^0_{n,\mathbf{k}} - \varepsilon^0_{n',\mathbf{k}+\mathbf{q}} + i\eta}\langle\varphi^0_{n,\mathbf{k}}|e^{-i(\mathbf{q}+\mathbf{G})\mathbf{r}}|\varphi^0_{n',\mathbf{k}+\mathbf{q}}\rangle\langle\varphi^0_{n',\mathbf{k}+\mathbf{q}}|e^{i(\mathbf{q}+\mathbf{G})\mathbf{r}}|\varphi^0_{n,\mathbf{k}}\rangle, \tag{5}$$

where $\varphi^0_{n,\mathbf{k}}, \varepsilon^0_{n,\mathbf{k}}, f_{n,\mathbf{k}}$ are respectively the unperturbed single-particle wavefunctions, their eigenvalues and occupation numbers, V is the volume of the unit-cell and n, n' are indices that span all of the occupied and unoccupied bands. The accurate calculation of χ in a wide frequency range using eq. (4) and (5) will require a separate calculation for each value of the frequency and knowledge of all of the empty states up to the requested energy, which makes this task cumbersome.

2.2. Sternheimer equations

On the other hand, the density response-function can be defined through the first-order correction to the density $n(\mathbf{r},t) = n^0(\mathbf{r}) + n'(\mathbf{r},t)$ of the system under a weak external perturbation $V_{ext}(\mathbf{r},t) = V^0_{ext}(\mathbf{r}) + V'_{ext}(\mathbf{r},t)$:

$$n'(\mathbf{r},t) = \int_{-\infty}^{\infty} dt' \int d\mathbf{r}' \chi(\mathbf{r},\mathbf{r}',t-t') V'_{ext}(\mathbf{r}',t'). \tag{6}$$

In the case of EEL spectroscopy, the external perturbation is $V'_{ext}(\mathbf{r}',t') \sim e^{i(\mathbf{q}\cdot\mathbf{r}-\omega t)}$. One can perform a direct calculation of the χ using density functional perturbation theory (DFPT) techniques without explicit calculation of empty states [9] and without solving the Dyson-like equation (4). In this framework a system under external perturbation can be described by the TDDFPT KS equation:

$$i\hbar \frac{\partial \varphi_{n,\mathbf{k}}(\mathbf{r},t)}{\partial t} = \hat{H}^{KS}(\mathbf{r},t)\varphi_{n,\mathbf{k}}(\mathbf{r},t), \tag{7}$$

where $\varphi_{n,\mathbf{k}}(\mathbf{r},t) = \varphi^0_{n,\mathbf{k}}(\mathbf{r}) + \varphi'_{n,\mathbf{k}}(\mathbf{r},t)$ is the KS wavefunction decomposed into the unperturbed KS wave and its first-order variation. $\hat{H}^{KS}(\mathbf{r},t) = \hat{H}^0(\mathbf{r}) + V'(\mathbf{r},t)$ is the KS Hamiltonian which consists in the static unperturbed Hamiltonian $\hat{H}^0(\mathbf{r})$ and of the (linearized) perturbation part $V'(\mathbf{r},t)$. This equation and its complex-conjugate can be linearized and, taking into account only the first-order response, yield the so-called Sternheimer equation [9] which, in the frequency domain, reads:

$$(\hat{H}^0 - \varepsilon^0_{n,\mathbf{k}} - \hbar\omega)\varphi'_{n,\mathbf{k}}(\mathbf{r},\omega) + \hat{P}_c V'_{Hxc}(\mathbf{r},\omega)\varphi^0_{n,\mathbf{k}}(\mathbf{r}) = -\hat{P}_c V'_{ext}(\mathbf{r},\omega)\varphi^0_{n,\mathbf{k}}(\mathbf{r}), \tag{8}$$

$$(\hat{H}^0 - \varepsilon^0_{n,-\mathbf{k}} + \hbar\omega)\varphi'^*_{n,-\mathbf{k}}(\mathbf{r},-\omega) + \hat{P}_c V'^*_{Hxc}(\mathbf{r},-\omega)\varphi^0_{n,\mathbf{k}}(\mathbf{r}) = -\hat{P}_c V'^*_{ext}(\mathbf{r},-\omega)\varphi^0_{n,\mathbf{k}}(\mathbf{r}), \tag{9}$$

where $\hat{P}_c$ is a projector on empty states and the first order correction to the density $n'(\mathbf{r},t)$ reads:

$$n'(\mathbf{r},t) = \sum_{\mathbf{k}}^{BZ} \sum_{n} \varphi^{0*}_{n,\mathbf{k}}(\mathbf{r}) \left[\varphi'^*_{n,-\mathbf{k}}(\mathbf{r},-\omega) + \varphi'_{n,\mathbf{k}}(\mathbf{r},\omega)\right] \tag{10}$$

where n now only spans the occupied bands. For metals, partially occupied bands should be accounted for using the smearing approach [10, 11]. However, for the sake of simplicity it is ommited in the present work, and only the insulating case is considered. This set of equations can be solved self-consistently for each value of ω, allowing us to obtain the susceptibility χ of the system.

2.3. The Liouville-Lanczos equation

Equivalently, instead of eq. (7), one can use the quantum Liouville equation [12, 13, 14]:

$$i\hbar \frac{d\hat{\rho}(t)}{dt} = \left[\hat{H}_{KS}(t), \hat{\rho}(t)\right], \tag{11}$$

where $\hat{\rho}(t)$ is the reduced one-electron KS density-matrix whose kernel reads:

$$\rho(\mathbf{r},\mathbf{r}',t) = \sum \varphi_v(\mathbf{r},t)\varphi^*_v(\mathbf{r}',t), \tag{12}$$

and $n(\mathbf{r},t) = \rho(\mathbf{r},\mathbf{r},t)$. Equation (11) can be linearized in the same manner as eq. (7), leading to the linearized Liouvillian equation:

$$(\hbar\omega - \hat{\mathcal{L}}) \cdot \hat{\tilde{\rho}}'(\omega) = \left[\tilde{V}'_{ext}(\omega), \hat{\rho}^0\right]. \tag{13}$$

The action of the Liouvillian superoperator $\hat{\mathcal{L}}$ onto $\hat{\rho}$ is defined as:

$$\hat{\mathcal{L}} \cdot \hat{\rho}' = \left[\hat{H}^0, \hat{\rho}'\right] + \left[V'_{Hxc}[\hat{\rho}'], \hat{\rho}^0\right]. \tag{14}$$

Equation (13) can be solved using the Lanczos recursive scheme for all of the frequencies at once, resulting in the susceptibility χ.

2.4. Comparison of the methods

Each of three methods briefly described in Sec. 2.1 to 2.3 allows us to perform a first-principle calculation of the linear density response function $\chi(\mathbf{q}, \omega)$ and, thus, to obtain the dielectric and loss function of a given system, that can be directly compared to the experimental measurements (see eq. (1)). Each method has advantages and drawbacks, the understanding of which is necessary to choose the approach the most adapted to the target-problem.

Calculation of χ using a Dyson-like equation [15] is a powerful method that allows one to access and analyze individual electronic excitations in the material. However, this information comes for a relatively high cost: computation of χ^0 in eq. (5) requires the computation of corresponding empty states, and computation of χ in eq. (4) involves multiplication and inversion of large matrices, making this calculations demanding in terms of central processing unit (CPU) time and random access memory (RAM).

On the contrary, usage of DFPT techniques [9] in the Sternheimer approach allows one to avoid the computation of the (numerous) empty states, by introducing the projector on the empty states $\hat{P}_c$ in eq. (8) and (9). This reduces the RAM and CPU time usage. Nevertheless, the CPU time usage will remain high for the calculation over a wide frequency range, as the self-consistent solution of eq. (8) and (9) should be repeated for each value of the desired frequency.

The Lanczos recursion algorithm used to solve the linearized Liouvillian equation (13) allows us to avoid the explicit computation of the susceptibility for each frequency value, separating the calculation into two steps. The first step of the Lanczos recursion is time consuming. It is used to generate a tridiagonal matrix of coefficients which is used in the second step (post-processing) to calculate the frequency-dependent susceptibility χ. This scheme allows one to reduce CPU time usage significantly. However, there are two main drawbacks of the Liouville-Lanczos approach: firstly, it is possible to perform calculations only in the case of an adiabatic exchange and correlation functional V'_{Hxc} in eq. (14). In the case where V'_{Hxc} has an explicit frequency dependence, one will have to repeat the recursive procedure for each desired value of the frequency, increasing the CPU time tremendously, therefore making this procedure inefficient. Secondly, within both Liouville-Lanczos and Sternheimer approaches, it is not possible to retrieve the information from which orbitals a specific peak in a spectrum consists of, thus making an analysis for understanding the physical origins more demanding.

3. Comparison of the results and performance of two codes: *turboEELS* and *thermo_pw*

3.1. Computational details

Ground state properties have been calculated using the density functional theory (DFT) [16, 17] in the plane wave and pseudopotential method within the local density approximation [18] for bismuth and the generalized gradient approximation [19] for gold.

For bulk Bi, a 2-atom trigonal unit-cell was used, with a plane wave basis set limited with a cutoff energy of 60 Ry. A Monkhorst-Pack grid of 14^3 **k**-points has been used to sample the Brillouin zone [20]. For the calculation of EEL spectra, a small transferred momentum of $\mathbf{q} = 0.013\text{Å}^{-1}$ in the (111) trigonal direction was chosen. An imaginary frequency was introduced, so that $\hbar\omega$ in eq. (8) and (9) reads $\hbar\omega + i\eta$, with $\eta = 0.135eV$. Indeed, the Sternheimer equations are solved with this broadening. At variance, in the Liouville-Lanczos method the broadening is

used only in the post-processing step, when the χ response function is built from the recursion coefficients. Calculations were performed using both scalar-relativistic - no spin-orbit coupling (SOC) and full-relativistic - with SOC normconserving pseudopotentials [21]. The number of iterations in the Lanczos recursion was 8000.

For bulk Au a 1-atom face-centered cubic unit-cell was used, with a plane wave basis set limited with a cutoff energy of 60 Ry. A Monkhorst-Pack grid of 32^3 **k**-points has been used to sample the Brillouin zone. For the calculation of EEL spectra, a small transferred momentum of $\mathbf{q} = 0.039\text{Å}^{-1}$ was used and an imaginary frequency $\eta = 0.135eV$ was added. Calculations were performed using scalar relativistic (without SOC) normconserving pseudopotential [22]. The number of iterations in the Lanczos recursion was 5000.

Convergence was carefully checked. In the *thermo_pw* the procedure has an explicit convergence threshold parameter on the variation of the density. This threshold was set to 10^{-12}. In the Liouville-Lanczos approach, the recursion chain should be cut after a certain number of iterations, meaning that convergence should be verified manually by performing additional iterations.

Both Sternheimer (*thermo_pw* code, unpublished [23]) and the Liouville-Lanczos (*turboEELS* code [14]) approaches are implemented in the QUANTUM ESPRESSO package for electronic structure calculations [24, 25]. Both codes support normconserving and ultrasolf pseudopotentials. Several levels of MPI parallelization are implemented: a plane-wave parallelization and a **k**-point parallelization.

3.2. Results

In figure 1, we report EEL spectra for bulk Bi obtained both with the *thermo_pw* code, and with *turboEELS*: results are in perfect agreement with each other and with previous calculations [3], both with and without SOC. We point out that the TDDFPT calculations were performed with, as input, data coming from the same (DFT) ground state self-consistent calculation.

Figure 2 shows the comparison of the EEL spectra for bulk Au obtained by *thermo_pw* and *turboEELS* codes.Obtained results are in agreement with previous ab initio calculations of the EELS for Au [26]. In the figure 2 one can see a severely damped plasmon peak around 2.5 eV and numerous interband transition at higher energies.

Figure 3 shows the relative difference between EEL spectra computed with the *thermo_pw* and *turboEELS* codes. Beyond 2 eV the agreement is perfect and the two codes agree within 1%. Below 2 eV, the loss function is tending to 0 and the magnitude of the relative difference becomes higher as the loss function does not tend to 0 in the same way. Indeed, oscillations that are intrinsic to the Lanczos, approach are magnified in the difference at low energy. As in the case for Bi, agreement is perfect, that indicates that both codes are well-suited to handle either semimetallic or metallic materials.

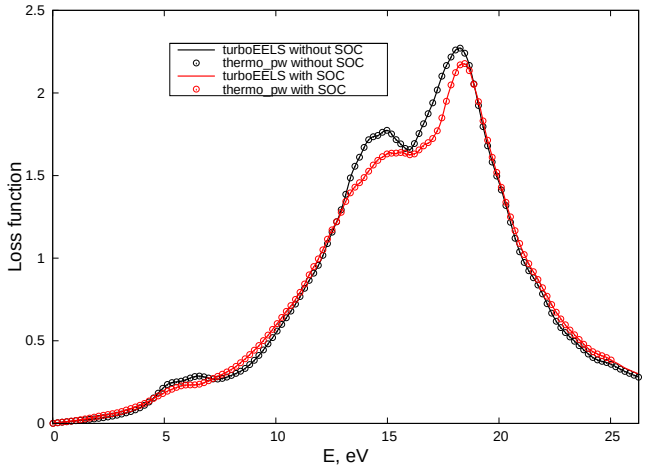

Figure 1: Bulk Bi. Loss function for a transferred momentum $\mathbf{q} = 0.013\text{Å}^{-1}$ in the z-direction obtained using: *turboEELS* code without (——) and with —— spin-orbit coupling (SOC), and *thermo_pw* code without (○) and with (○) SOC.

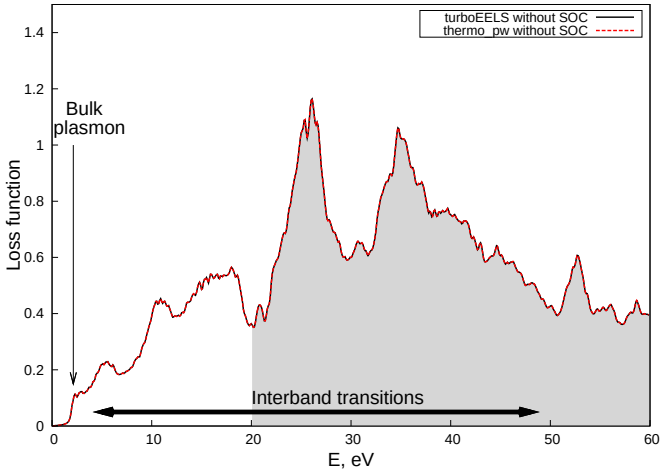

Figure 2: Bulk Au. Loss function for a vanishing transferred momentum is the x-direction, calculated with the *turboEELS* code (——) and *thermo_pw* code (- - - -). Shaded area marks the energy region where our pseudopotential is less accurate and arrows indicate the position of bulk plasmon and the region on interband transitions.

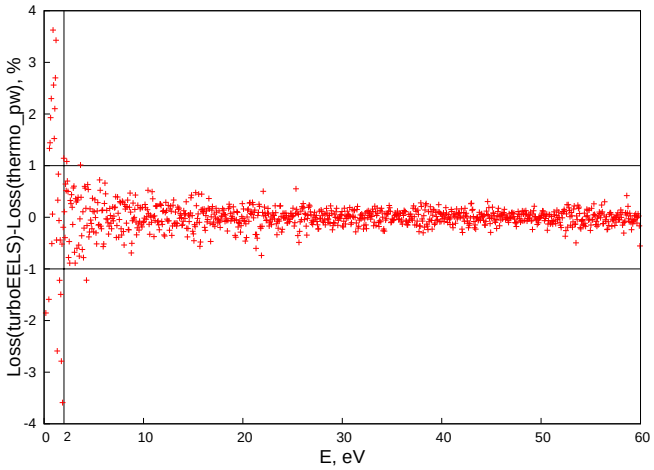

Figure 3: Bulk Au. Relative difference between the loss functions computed for a vanishing transferred momentum is the x-direction, calculated with the *turboEELS* and *thermo_pw* codes.

3.3. Performance

In figure 4, we show the comparison of the performance of both codes in terms of CPU time for bulk Bi without SOC. One can see that the *turboEELS* code is more efficient than the *thermo_pw* code on a wide frequency range. We note that calculations in a low frequency region (0-10 eV) are considerably faster, by a factor of 2-3, than in the middle and high frequency region (10-30 eV).

In table 1, we show the amount of time, number of CPU cores and number of frequencies used

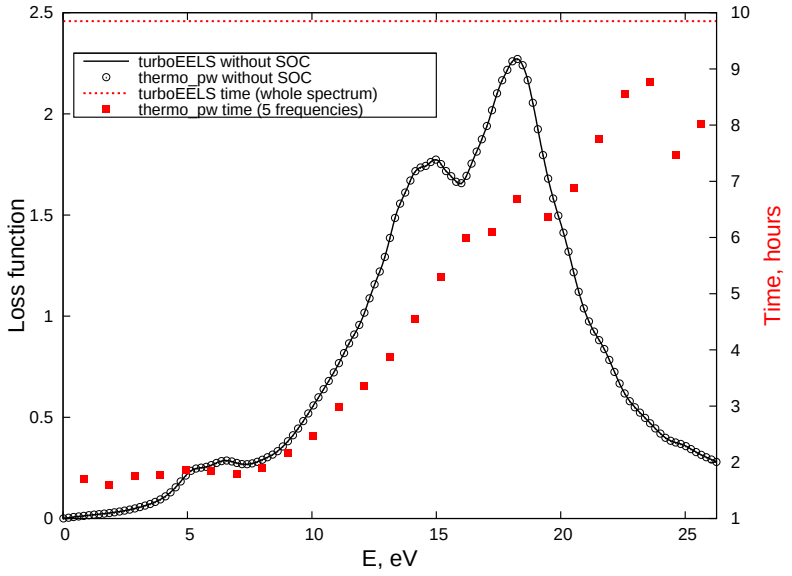

Figure 4: Bulk Bi. Performance comparison of *turboEELS* and *thermo_pw* codes without spin-orbit coupling. Loss functions obtained with *turboEELS* (——) and *thermo_pw* (○) codes are shown (left-hand side abscissa). Time required for *turboEELS* (- - - -) to compute the whole spectrum and for *thermo_pw* (■) to compute the loss function for five frequencies in the corresponding frequency range is shown (right-hand side abscissa).

to obtain curves in fig. 2 and 4. In the last column of table 1, the number of frequency is given, showing on average how many frequencies can be calculated with *thermo_pw* when consuming the same amount of CPU time needed for *turboEELS* to calculate the whole spectra. We point out that the *ratio* may however depend on the selected frequency range.

Performance comparison for the calculation with SOC is not shown in the present work. Taking SOC into account roughly increases the required CPU time by a factor of 4 for both codes, without influencing their relative performance.

Table 1: Performance comparison of the *turboEELS* and *thermo_pw* codes for bulk Bi and Au.

System	# of CPU cores	# of frequencies (ω)	Time (h)	average # of ω for *thermo_pw* to match *turboEELS* CPU time
Bi *turboEELS*	72	any	10	
Bi *thermo_pw*	72	130	118	11
Au *turboEELS*	240	any	0.75	
Au *thermo_pw*	240	600	16	28

4. Conclusions

In this work we have done a comparison between results and performance of the codes and corresponding methods that allow us to calculate EEL spectra. It has been found that results obtained using the Sternheimer equation and the Liouville-Lanczos approach are in perfect agreement with each other for semiconducting (not shown), semimetallic and metallic samples.

However, as anticipated in Sec. 2.4, the performance of the *turboEELS* code is significantly better when the range of frequencies is wide. In principle it is possible to calculate EEL spectra on a 0-250 eV range at the same computational cost as on the 0-25 eV interval, although it might be necessary to include core electrons in the pseudopotential in order to describe high-energy excitations correctly. One can see that it is convenient to use the *thermo_pw* code for a precise calculation of the susceptibility in a narrow frequency range.

Acknowledgement
Calculations have been performed with the QUANTUM ESPRESSO packages [25]. Support from the ANR-10-LABX-0039-PALM program (Femtonic project), from the DGA (France), from the program NEEDS-Matériaux (France) and from the Chaire Énergie of the École Polytechnique is gratefully acknowledged. Computer time was granted by École Polytechnique through the LLR-LSI project, by GENCI (Project No. 2210) and by PRACE (Project No. 2010PA3750). Andrea Dal Corso acknowledges support from the European Union H2020-EINFRA-2015-1 programme under grant agreement No. 676598 project "MaX - materials at the exascale".

References

[1] Egerton R F 1996 *Electron Energy-Loss Spectroscopy in the Electron Microscope* 2nd ed (New York and London: Plenum)
[2] Botti S, Schindlmayr A, Sole R D and Reining L 2007 *Rep. Prog. Phys.* **70** 357
[3] Timrov I, Markov M, Gorni T, Raynaud M, Motornyi O, Gebauer R, Baroni S and Vast N 2017 *Phys. Rev. B* **95** 094301
[4] See in particular Ref. 9-14 and 28-48 of Ref. [3]
[5] Olevano V and Reining L 2001 *Phys. Rev. Lett.* **86** 5962
[6] Runge E and Gross E 1984 *Phys. Rev. Lett.* **52** 997
[7] Gross E K U and Kohn W 1985 *Phys. Rev. Lett.* **55** 2850
[8] Car R, Tosatti E, Baroni S and Leelaprute S 1981 *Phys. Rev. B* **24** 985
[9] Baroni S, de Gironcoli S, Corso A D and Giannozzi P 2001 *Rev. Mod. Phys.* **73** 515
[10] de Gironcoli S 1995 *Phys. Rev. B* **51** 6773
[11] Methfessel M and Paxton A 1989 *Phys. Rev. B* **40** 3616
[12] Rocca D, Gebauer R, Saas Y and Baroni S 2008 *J. Chem. Phys.* **128** 154105
[13] Timrov I, Vast N, Gebauer R and Baroni S 2014 *Phys. Rev. B* **88** 064301
[14] Timrov I, Vast N, Gebauer R and Baroni S 2015 *Computer Physics Communications* **06/2015** dOI: 10.1016/j.cpc.2015.05.021
[15] Onida G, Reining L and Rubio A 2002 *Rev. Mod. Phys.* **74** 601
[16] Hohenberg P and Kohn W 1964 *Phys. Rev.* **136** B864
[17] Kohn W and Sham L 1965 *Phys. Rev.* **140** A1133
[18] Perdew J P and Zunger A 1981 *Phys. Rev. B* **23** 5048
[19] Perdew J, Burke K and Ernzerhof M 1996 *Phys. Rev. Lett.* **77** 3865
[20] Monkhorst H and Pack J 1976 *Phys. Rev. B* **13** 5188
[21] Markov M, Sjakste J, Fugallo G, Paulatto L, Lazzeri M, Mauri F and Vast N 2016 *Phys. Rev. B* **93** 064301
[22] Pseudopotential was generated using parameters provided in `http://bohr.inesc-mn.pt/~jlm/pseudo.html`
[23] Code can be obtained from `http://people.sissa.it/~dalcorso/thermo_pw_dist.html`
[24] Giannozzi P, Baroni S, Bonini N, Calandra M, Car R, Cavazzoni C, Ceresoli D, Chiarotti G, Cococcioni M, Dabo I, Dal Corso A, De Gironcoli S, Fabris S, Fratesi G, Gebauer R, Gerstmann U, Gougoussis C, Kokalj A, Lazzeri M, Martin-Samos L, Marzari N, Mauri F, Mazzarello R, Paolini S, Pasquarello A, Paulatto L, Sbraccia C, Scandolo S, Sclauzero G, Seitsonen A, Smogunov A, Umari P and Wentzcovitch R 2009 *J. Phys.: Condens. Matter* **21** 395502
[25] Giannozzi P, Andreussi O, Brumme T, Bunau O, Nardelli M B, Calandra M, Car R, Cavazzoni C, Ceresoli D, Cococcioni M, Colonna N, Carnimeo I, Corso A D, de Gironcoli S, Delugas P, Ferretti R A D J A, Floris A, Fratesi G, Fugallo G, Gebauer R, Gerstmann U, Giustino F, Gorni T, Jia J, Kawamura M, Ko H Y, Kokalj A, Küçükbenli E, Lazzeri M, Marsili M, Marzari N, Mauri F, Nguyen N L, Nguyen H V, de-la Roza A O, Paulatto L, Poncé S, Rocca D, Sabatini R, Santra B, Schlipf M, Seitsonen A P, Smogunov A, Timrov I, Thonhauser T, Umari P, Vast N, Wu X and Baroni S 2017 *J. Phys.: Condens. Matter* **29** 465901 URL `http://www.quantum-espresso.org`
[26] Alkauskas A, Schneider S D, Hébert C, Sagmeister S and Draxl C 2013 *Phys. Rev. B* **88** 195124